Pham DQ *et al.* (2025)
Notulae Botanicae Horti Agrobotanici Cluj-Napoca
Volume 53, Issue 1, Article number 14108
DOI:10.15835/nbha53114108
Research Article

Antifungal nanoformulation of botanical anthraquinone and TiO_2 against melon phytopathogenic fungi: preparation, *in vitro* bioassays and field test

Duong Quang PHAM[1,2], Tan Van CHU[1], Hiep Thi PHAN[3], Son Vu NGUYEN[3], Tam The LE[4], De Quang TRAN[5], Hung Khac NGUYEN[1], Anh Thi Kieu VO[2,6], Lam Dai TRAN[2,6], Khanh Ngoc TRAN[7], Hoang Dinh VU[3]*, Quang Dang LE[2,6]*

[1]*Vietnam Academy of Science and Technology (VAST), Center for High Technology Research and Development, 18 Hoang Quoc Viet, Hanoi 10072, Vietnam; quangduongpham@gmail.com (D.Q.P); tanbkhnk44@gmail.com (T.V.C); hungkhacibt@gmail.com (H.K.N)*
[2]*Vietnam Academy of Science and Technology (VAST), Institute for Tropical Technology, 18 Hoang Quoc Viet, Hanoi 10072, Vietnam; vothikieuanh2013@gmail.com (A.T.K.V); ledangquang2011@gmail.com; ldquang@itt.vast.vn (*corresponding author) (Q.D.L); trandailam@gmail.com (L.D.T)*
[3]*Hanoi University of Science and Technology, School of Chemistry and Life Sciences, 1 Dai Co Viet, Hanoi 10000, Vietnam; Hiep.pt0311@gmail.com (H.T.P); nvson0710@gmail.com (S.V.V); hoang.vudinh@hust.edu.vn (*corresponding author) (H.D.V);*
[4]*Vinh University, Vinh City, Nghe An 460000, Vietnam; tamlt@vinhuni.edu.vn (T.T.L)*
[5]*Can Tho University, College of Natural Sciences, Department of Health Sciences, Can Tho 94000, Vietnam; tqde@ctu.edu.vn (T.Q.D)*
[6]*Graduate University of Science and Technology, Vietnam Academy of Science and Technology (VAST), 18 Hoang Quoc Viet, Hanoi 10072, Vietnam*
[7]*Vietnam Academy of Agricultural Sciences, Plant Protection Research Institute, Division of Pathology & Phyto-Immunology, Hanoi 10000, Vietnam; ngockhanh2301@gmail.com (K.N.T)*

Abstract

Anthraquinones from *Polygonum cuspidatum* are well-known antimicrobial botanical compounds against several plant pathogenic agents that cause plant disease. In this study, for the first time, the anthraquinone-rich extract of *P. cuspitaum* and TiO_2 nanoparticles (average droplet size of 103.9 nm) together with surfactants and cosurfactants were fabricated in the type of emulsifiable concentrate (ATEC) that form spontaneous nanoemulsions (ATNE) in water and evaluated its antifungal efficacy against the melon fungal diseases. The morphology of ATNE nanodroplets observed using SEM and TEM showed that ATNE droplets were spherical in shape. ATEC showed excellent antifungal activity against various melon phytopathogenic fungi. At a concentration of 0.5%, the formulation completely inhibited the mycelial growth of *Botrytis cinerea*, *Phytophthora* spp., *Fusarium oxysporum*, *Colletotrichum* spp., *Sclerotium* spp., and *Rhizoctonia* spp., and the germination of *Eryshipe cichorasearum* spores. In the field test, ATNE nanoformulations were evaluated for their control efficacy against powdery mildew by spraying on young honeydew melon plants. As a result, ATNE (1:400) with an average droplet size of 484.4 nm exhibited the best suppression (control efficacy of 62.34 %)

Received: 06 Sep 2024. Received in revised form: 04 Dec 2024. Accepted: 20 Jan 2025. Published online: 25 Feb 2025.
From Volume 49, Issue 1, 2021, Notulae Botanicae Horti Agrobotanici Cluj-Napoca journal uses article numbers in place of the traditional method of continuous pagination through the volume. The journal will continue to appear quarterly, as before, with four annual numbers.

against powdery mildew at 10 days after spray and showed no phytotoxicity on the test plants. The study results confirmed the potential of ATEC against various melon phytopathogenic fungi. In particular, under organic agriculture practice, the nanoemulsion ATNE could effectively control powdery mildew caused by *E. cichorasearum* in honeydew melon fields.

Keywords: anthraquinone; antifungal activity; field test; melon; nanoemulsion; TiO_2 nanoparticles

Introduction

Honeydew melon belongs to melon (*Cucumis melo* L.), a type of true melon from the family Cucurbitaceae. Currently, they have been cultivated widely in numerous agricultural areas to produce high-value fruit products in Vietnam. However, the quality and fruit production yield of melons are affected by various pests insects, and diseases. Among the fungal diseases, Fusarium wilt, powdery mildew, downy mildew, Alternaria leaf blight, and leaf blight are common phytopathogenic agents (Cui *et al*., 2022). Fusarium wilt, caused by *Fusarium oxysporum* f.sp. *melonis*, downy mildew caused by *Pseudoperonospora cubensis*, and powdery mildew caused by *Eryshipe cichorasearum*, have been reported to cause severe damage to melon plants (Cui *et al*., 2022; Elagamey *et al*., 2023). *Pseudoperonospora cubensis*, and *Eryshipe cichorasearum* infect melons in many countries including Vietnam and Southeast Asia (Chung *et al*., 2022). Both the mature plant and seedling stages of *Cucumis melo* Inodorus plants are susceptible to the two fungi. In the Northern provinces of Vietnam, the honeydew melon cultivar Kim Co Nuong (KCN) has been widely cultivated. *Eryshipe cichorasearum* which causes powdery mildew and *P. cubensis* which causes downy mildew are common and main pathogenic fungi that affect KCN honeydew melon; they are also infective in various stages of melon development and cause severe losses of the fruit production in this crop (Chung *et al*., 2022). In Northern parts of Vietnam, powdery mildew and downy mildew infections are found commonly from spring to summer (Dinh *et al*., 2021). Besides, the control for powdery mildew and downy mildew in honeydew melon has been mostly used chemical synthetic fungicides such as azoxystrobin, dimethomorph, chlorothalonil, and mancozeb (Dinh *et al*., 2021). Those chemical fungicides have effectively controlled plant diseases. However, their residues that may link to health concerns for pesticide handlers, and long-term toxic effects on humans through food contamination and environment have been warned (Mostafa *et al*., 2021). In an organic agriculture practice, the use of synthetical fungicides is also limited or phased out. There are many researches on biofungicides and biorational fungicides to find alternatives for harmful fungicides, but the application of the biofungicides has been limited in the control of fungal plant pathogens in honeydew melon. Several nanoemulsions of botanicals such as plant extracts, plant oils and essential oils that fabricated and showed antifungal activity against plant pathogenic fungi (Azmi *et al*., 2022). Natural essential oils from plants (lavender, peppermint, lemon, orange, cinnamon, clove, oregano, thyme, basil, and mustard) are reported by the United States Food and Drug Administration to have a "Generally Recognized as Safe" (GRAS) status and are approved to use in food industry (Elsalam and Khokhlov, 2015; Mostafa *et al*., 2021; Pandey *et al*., 2017;). Therefore, nanoemulsions of essential oil could be seen as a green approach in plant protection. Nanoformulations of clove and black seed essential oils (2:1) effectively inhibited conidia sporulation of melon fungal pathogens *Galactomyces candidum*, *Alternaria tenuissima* and *Fusarium solani* (Mossa *et al*., 2021). Elsalam and Khokhlov (2015) prepared nanoemulsion of eugenol from essential oil, surfactant and water, which had particle sizes ranging from 50 to 120 nm and at a concentration of 2% completely inhibited the mycelial growth of all strains of *Fusarium oxysporum* f. sp. *vasinfectum*. Limonin-loaded eugenol nanoemulsion (245.7 nm) showed a MIC of 160 μg/mL against *Penicillium italicum* (Yi *et al*., 2021). Despite that several nanoformulations of natural products have been

investigated on antifungal activity against fungal pathogens, to date, no studies have been focused on the use of nanoformulation to control melon fungal pathogens such as powdery mildew and downy mildew.

Recently, several botanical anthraquinones have been described in their antifungal activity against phytopathogenic fungi. Emodin, physcion, aloe-emodin, and rhein isolated from the chloroform fraction of *Cassia tora* seeds showed strong to moderate fungicidal activities against *B. cinerea*, *E. graminis*, *P. infestans*, and *R. solani*. The phytochemical anthraquinone extract containing physcion and chrysophanol derived from *Rumex chinensis* roots showed high in vivo antifungal efficacy against wheat leaf rust and barley powdery mildew (Pham *et al*., 2020).

The medicinal plant, *Polygonum cuspidatum* (also known as *Reynoutria japonica*, or *Fallopia japonica*) is a species of herbaceous perennial plant in the knotweed and buckwheat family Polygonaceae. The root extracts of *P. cuspidatum* have been known to be rich in emodin and physcion and displayed various biological activities such as antimicrobial activity, and antioxidant and anti-inflammatory properties (Ke *et al*., 2023). Besides, 1,8 dihydroxyanthraquinones have been known for their ability to photosensitize TiO_2 and promote the photodynamic inactivation of microorganisms by TiO_2 (Trochowski *et al*., 2023).

TiO_2 nanoparticles (TiO_2 NPs) can promote plant growth and productivity, reduce biotic stress, and trigger plant resistance to fungal infection (Satti *et al*., 2022; Vatankhah *et al*., 2023). TiO_2 nanoparticles displayed significant antimicrobial activity against plant bacterium *Xanthomonas phaseoli* and fungi such as *F. oxysporum*, *Rhizoctonia solani*, and *Sclerotium rolfsii* (Ali Alasmary *et al*., 2022). Other metal NPs such as silver NPs biosynthesized by *Rhazya stricta* leaf extract significantly inhibited the pathogenic fungi *Drechslera halodes*, *D. tetramera*, *Macrophomina phaseolina*, *Alternaria alternata*, and *Curvularia australiensis* (Al-Sahli *et al*., 2024). In the previous studies by Arezoo *et al*. (2020) and Saka *et al*. (2022), the incorporation of TiO_2 NPs with botanical extracts led to an enhancement of the antimicrobial properties of the resulting formulation. TiO_2 NPs biosynthesized through Carica-papaya shell extracts displayed antifungal influence and controlled the reproductions of *Sclerotinias sclerotiorums*, *Fusarium* spp, and *Rosellinia necatrixs* (Saka *et al*., 2022). Sago starch films' functional characteristics were enhanced by the incorporation of TiO_2 NPs and cinnamon essential oil, which demonstrated excellent antibacterial activity against *Salmonella typhimurium*, *Escherichia coli*, and *Staphylococcus aureus* (Arezoo *et al*., 2020). TiO_2 NPs in anatase and rutile forms with surface modification by geraniol (plant monoterpen) also demonstrated a notable reduction in the biofilm thickness of methicillin-resistant *S. aureus* (Younis *et al*., 2023). However, a hypothesis of creating a nanoformulation consisting of two components TiO_2 NPs and bioactive anthraquinones that will produce high antifungal potent against plant fungal pathogens has never been researched.

Our study objectives are to fabricate a novel and unique nanoemulsion with available and common green materials, such as anthraquinone-rich extract from *P. cuspidatum* roots, and TiO_2 NPs as active ingredients, and the by-product of cinnamon oil as an additive, to characterize the resultant nanoemulsion, and to evaluate for their antifungal activity against melon phytopathogenic fungi by in vitro bioassay and field test. The research results could create an eco-friendly type of nanoformulation that effectively controls fungal plant pathogens in melon.

Materials and Methods

Botanical anthraquinone extraction, fractionation and isolation

The specimen of *P. cuspidatum* roots was identified by Dr. Quang Duong Pham and stored in CHTD. The dried and ground materials of *P. cuspidatum* roots (2.5 kg) were refluxed and extracted with 6 L of methanol for 24h. The extract was then filtered through a filter paper to collect the total methanol extract. This methanol extract was evaporated to obtain 450 (g) of methanol residue. The methanol residue was

dispersed in water and partitioned with ethyl acetate (EtOAc) to give EtOAc extract; it was further extracted with n-hexane to give an extract rich in anthraquinone. The main anthraquinone in the anthraquinone-rich extract was purified by column chromatography and quantitatively analyzed by HPLC. A portion of 10 g of the n-hexane extract was separated on a silica gel chromatographic column (60 g, particle size 0.04-0.063 mm, D 30 mm × L 500 mm). The elution solvent system was n-hexane: EtOAc (v/v: 90:10-70:30), giving 5 fractions. Compound CKC1 (5 mg) was obtained as red crystals in fraction 3. The chemical structure of CKC1 was identified by ^{1}H and ^{13}C-NMR (Supporting information). The content of CKC1 was quantified by HPLC using Agilent 1100 Infinity II High-Performance Liquid Chromatography system with a C18 hydrosphere column (4.6 × 250 mm). The solvent system used was H_2O (40%), and ACN (60%). Temperature was 30 °C and 1 µL of injection was used. The flow rate was set at 0.5 mL/min and a DAD detector was employed to detect the peak of CKC1 at 223 nm, 258 nm, and 288 nm, respectively.

Preparation of TiO_2 nanoparticles

Titanium isopropoxide (TTIP: $Ti[OCH(CH_3)_2]_4$), ethanol (Xilong Scientific Co.Ltd, China), PEG 400 (TNJ Chemical, China), and distilled water were used for the preparation of TiO_2 nanoparticles. Firstly, solution A was made by dissolving TTIP in 50 mL of EtOH. In order to make solution B, 100 mL of PEG 400 was dissolved in 50 mL of EtOH and H_2O. Solution B was loaded into the reaction vessel. Secondly, simultaneously and gradually, solution A was added to the reaction vessel, which was placed in an ultrasonic bath with a frequency of 37 kHz, maintaining a temperature of 80 °C during the mixing process. The mixture was subjected to a continuous heating and ultrasonic process, followed by 15 h of ultrasonication to eliminate EtOH and produce TiO_2 NPs coated with PEG 400.

Preparation of emulsifiable concentrate and nanoemulsion of anthraquinone and TiO_2 NPs

An anthraquinone and TiO_2 NPs loaded emulsifiable concentrate (ATEC) was prepared using an anthraquinone-rich extract of *P. cuspidatum*, TiO_2 NPs, surfactants, and cosurfactants (Huang *et al*., 2024; Bui *et al*., 2021). Firstly, mixture 1 was composed using an anthraquinone-rich extract of *P. cuspidatum* (1811 mg) that was dissolved in propylene glycol (PG; 25 mL) and the by-product of cinnamon oil as an additive (25 mL) containing 13.9% of cinnamaldehyde (Provided by TECH-VINA Joint Stock Company, Vietnam). Mixture 1 was stirred for 15 min at 450 rpm to form the homogenation stage. Tween 20 (Guangdong Guanghua Sci-Tech Co.Ltd, China) (25 g) and Tween 60 (Guangdong Guanghua Sci-Tech Co.Ltd, China) (25 g) were successively added to mixture 1 under stirring at 450 rpm for 30 min and ultrasonicated at 20kHz for 15 min to make mixture 2. Secondly, 400 mg of TiO_2 NPs was added to mixture 2 and the obtained mixture was stirred at 450 rpm for 30 min to form ATEC. The characteristics of ATEC were determined by FTIR and its antifungal activity was evaluated against melon pathogenic fungi *in vitro*. The FTIR analysis was performed according to the method by Le *et al*. (2024).

Finally, the anthraquinone and TiO_2 NPs loaded nanoemulsion (ATNE) was prepared by dispersing the ATEC in water at the ratio of 1:400 and 1:700 using a stirrer at 450 rpm and ultrasonication for 15 min. The resulting nanoemulsion ATNE was measured for its droplet sizes, morphology, and stability by DLS and SEM.

Characterization of nanoformulation containing anthraquinone and TiO_2

The bondings of functional groups in the anthraquinone-rich extract, TiO_2 coated by PEG400 and ATEC were analyzed by Fourier transform infrared spectroscopy FT-IR (Bruker Tensor 27, Germany). The size distribution and stability of TiO_2 nanoemulsion with a coating layer of PEG400 and nanoemulsion ATEN were examined by dynamic light scattering (DLS) (Horiba SZ-100, Japan). Before measurement, ATNE diluted in water at a concentration of 100-fold dilution was used for characteristic analysis.

The morphology (size and shape) of the droplets of nanoemulsions was obtained by scanning electron microscopy (SEM - ZEISS EVO, Germany). The samples were diluted with water (1/2000, v/v), placed on a glass slide, and dried in a vacuum oven at room temperature. The surface of the dried nanoemulsion was coated with a layer of gold and palladium using a sputter coating technique. Then, scanning electron microscopy (SEM) images of ATEN were captured at various magnifications of 3,000×; 5,000× and 15,000×.

ATNE nanoemulsion droplet morphology was also examined using TEM (JEM- 2100, JEOL, Japan). After diluting the ATNE (1:400) nanoemulsion with water, it was applied to a copper grid covered in a carbon layer and allowed to dry before observing by TEM.

In vitro antifungal bioassay against fungal pathogens causal agents of melon

The resulting nanoemulsion formulations were tested with fungi grown in Potato dextro Agar (PDA) medium, monitoring fungal inhibition and comparing with the negative control after 2-5 days. The test fungi *Botrytis cinerea*, *Phytophthora* spp., *Fusarium oxysporum*, *Colletotrichum* spp., *Sclerotium* spp., and *Rhizoctonia* spp. which were isolated from melon-infected tissues were provided from Plant Protection Research Institute (PPRI). The PDA medium was autoclaved and cooled to about 50 °C, then the test sample was added. The ATSE was incorporated with melt PDA to form the treated media at test concentrations ranging from 0.125 % to 0.5 % ATEC. The resulting PDA was poured into a 9 cm diameter Petri dish. Three replicate Petri dishes were used for each nanoemulsion formulation. Three PDA dishes without nanoemulsion were used as negative controls (control samples). The positive controls were treated with SCORE 250EC (Syngenta, Vietnam). The inhibitions ATEC against test fungi were observed at 2, 4, and 6 days after inoculation. The fungal diameter was monitored and measured using an electronic caliper. The fungal inhibition efficiency was calculated according to the formula:

$$I\,(\%) = \frac{D_C - D_t}{D_C - 5} \times 100\%$$

where: D_C: Diameter of fungal mycelia on a negative control petri dish (mm); D_t: diameter of fungal mycelia on dish treated with nanoemulsion (mm); and 5: diameter of agar plug (mm).

In vitro tests of the antifungal effect of ATEC against *Erysiphe cihoracearum* were conducted in onion skin based on the test described by Hirata (1942). The onion was sliced into 1.5 cm by 1.5 cm pieces, peeled the onion into layers, and used a knife to separate the inner membranes. Ethanol 70° was dropped the onion membranes into and left for 1 week to remove the pungent smell of the onion. Before using the onion membranes, put it in a measuring tube, cover it with gauze, and rinse it under running water for 2 hours. Using tweezers, the onion membrane was removed and placed on the slide. A portion of the infected area was then cut and placed on the onion's surface. Pressure was then applied to cause the spores to fall into the onion membrane, and the onion membrane was then allowed to float on the water's surface in a petri dish based on various concentrations. The spore germination rate was measured and calculated (one hundred spores were counted for every concentration) (Hirata, 1942; Thanh, 2015).

Field test of ATNE against Erysiphe cihoracearum causing powdery mildew disease on honeydew melon

The disease control efficacy of ATNE was evaluated against honeydew melon powdery mildew disease (*E. cihoracearum*) was performed following Vietnam National Standard on Pesticides - Bio-efficacy field trials number TCVN 12561:2022 and Vietnam Sector Standard number 10TCN 333:1998. In brief, field trials of honeydew melons were conducted from March to June of 2024 in Hai Phong province (20.74° N; 106.73° E). The experiment was arranged in a completely randomized block in 4 experimental plots (30 m^2 each) of 4-week honeydew melon plants (KCN cultivar) and the experiment was conducted in triplicate (Vietnam Sector Standard No. 10TCN 333:1998). The honeydew melon plants were treated with ATNE nanoemulsions at the ratios of (1: 400) and (1:700), respectively. *Cheatomium* sp. (10^9 CFU/ml) was used as a positive control, and tap water was sprayed as a negative control. The plots were incorporated with a compost of organic materials (Nghiem T.Tam melon farm, Hai Phong, Vietnam) before planting, and fertilizer rates of 100-500 kg ha^{-1} of

12N–12P–17K were employed for melon cultivation. Environmental factors that were present when the melons were planted included soil pH of 6.0, relative humidity of 85–85%, and temperatures between 26 and 37 °C. Five random points of two diagonals in each plot were selected for plant disease assessments on the 5th and 10th day after the treatment. These points should be at least 1 meter or 1 row away from the plot edges. All leaves of three vines from each point were used for calculating disease incidence (DI) and disease severity index (DSI). DI index was calculated as follows: DI (%) = (Number of diseased leaves / Total number of leaves assessed) × 100. DSI was determined based on a 5-point scale of leaf disease syndrome and was measured as [(n1 × 1 + n2 × 2 + n3 × 3 + n4 × 4 + n5 × 5) × 100]/(5 × total number of the observed leaves), where n1–n5 are the numbers of observed melon leaves relative to the disease indices 1–5 (Table 1).

Table 1. Disease scoring scale of honeydew leaves infected with *E. cihoracearum*

Score	Percentage of leaf area damaged by *E. cihoracearum*
0	No disease syndrome
1	Below < 1% of infection lesions on the leaves observed
2	1 – 10% of infection lesions on the leaves observed
3	10 – 25% of infection lesions on the leaves observed
4	25 – 50% of infection lesions on the leaves observed
5	> 50 % of infection lesions on the leaves observed

Based on the Henderson-Tilton formula, the disease control efficacy was stated as a percentage as follows: Control efficacy (%) = (1- [(Ta×Cb)/(Ca×Tb)])×100, where: T_b and T_a are the DSI values of leaves in the treatment plot before and after spraying ATNE, respectively; C_b and C_a are the DSI of leaves in the negative control plot before and after spraying with tap water, respectively (Vietnam Sector Standard No. 10TCN 333:1998; Vietnam National Standard No. TCVN 12561:2022).

Statistical analysis

The in vitro experiments were performed at least in triplicate and data are expressed as the average value ±SD. Statistical analysis of biological testing data was performed based on ANOVA analysis using IRRISTAT 5.0. The statistical significance was determined at $p < 0.05$ based on the Least Significant Difference (LSD) test.

Results and Discussion

Constituents of the anthraquinone-rich extract of Polygonum cuspidatum roots

The anthraquinone-rich extract was prepared by a liquid-liquid partitioning of ethanol extract from *P. cuspidatum* roots. The n-hexane fraction and EtOAc fraction obtained by the partitioning were determined to contain a high content of anthraquinone. The anthraquinones isolated from EtOAc fraction of *P. cuspidatum* roots were identified as physcion, emodin, physcion-8-O-β-D-glucopyranoside, and emodin-8-O-β-D-glucopyranoside based on ESI-MS and ^{1}H and ^{13}C-NMR spectroscopy (Supporting information). The main anthraquinone compound isolated from n-hexane fraction was identified to be emodin based on the same spectroscopic techniques (Supporting information). The content of emodin was qualified by the HPLC method (Figure 1A). The HPLC analytical result showed that the content of emodin in n-hexane fraction and EtOAc fraction were 31.4 and 0.72%, respectively (Supporting information). Consequently, the n-hexane fraction was used as the active ingredient to further formulate an emulsifiable concentrate.

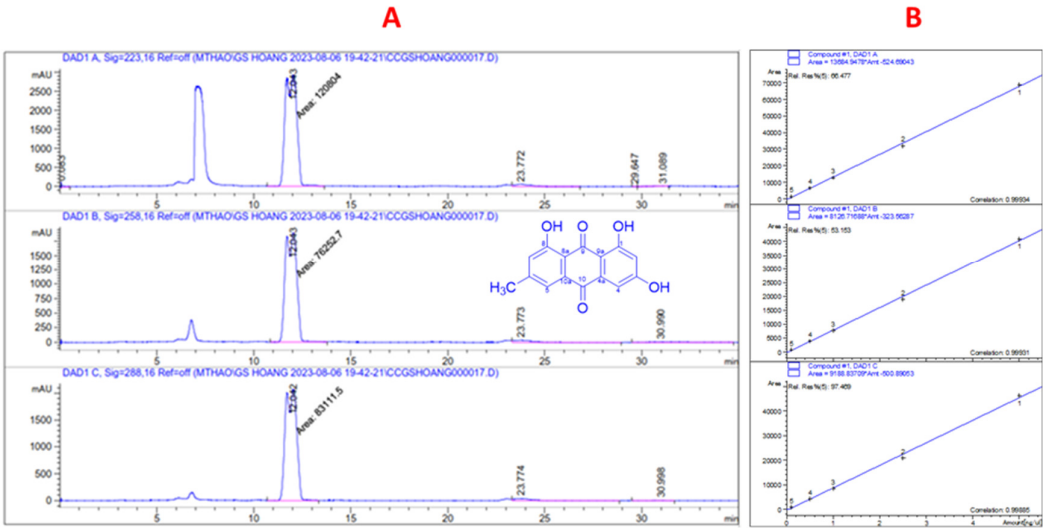

Figure 1. HPLC chromatograms of the anthraquinone-rich extract and structure of emodin

A: emodin (Rt = 12.1 min) in the anthraquinone-rich extract of *P. cuspidatum* roots (Detector DAD at 223 nm, 258 nm, and 288 nm; top to bottom, respectively) B: Calibration curves of emodin in the anthraquinone-rich extract that monitored at 223 nm, 258 nm, and 288 nm; top to bottom, respectively

Characterization of TiO_2 nanoparticles

TiO_2 nanoparticles were fabricated in the type of nanoemulsion with a coating layer of PEG400 using the sol-gel method. The suspension of TiO_2 NPs was characterized by DLS at the dilution of 2000 folds. The droplet size distribution of TiO_2 nanoparticles was recorded and the mean of droplet sizes was 103.9 nm as illustrated in Figure 2. PDI value of 0.284 suggested a narrow distribution with a high homogeneity for the colloidal system. The zeta potential (ζ = -62.2 mV) of the suspension of TiO_2 NPs (Figure 2B) indicated that the stability was good. The characteristics of small droplet size, high homogeneity, and good stability of TiO_2 NPs could be deduced from the synthesis using ultrasonic homogenization. Because ultrasound waves created the liquid's cavitation bubbles, the stability of the emulsions was attributed to the ultrasonic homogenization process.

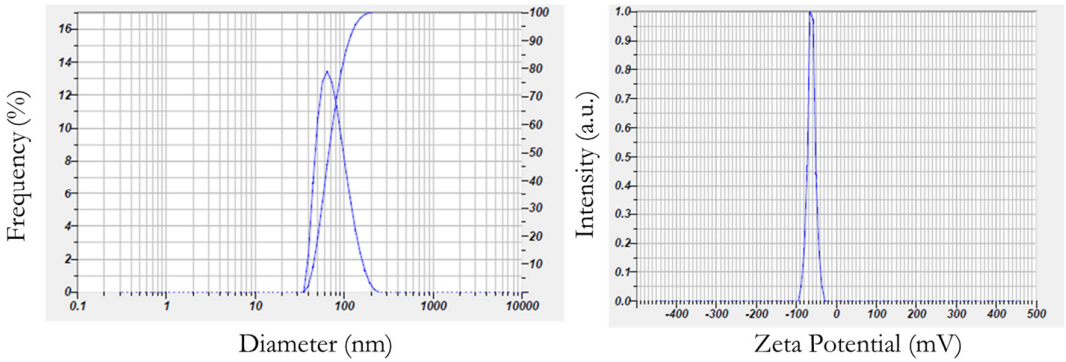

Figure 2. DLS measurement of the distribution of droplet sizes (a) and ζ potential (b) of TiO_2 nanoparticles

Characterization of emulsifiable concentrate and nanoemulsion of anthraquinone and TiO_2 NPs

Emulsifiable concentrate (EC) is a universal type of formulation that allows to formation of a spontaneous emulsion when mixed with water. Emulsifiable concentrate formulations generally contain high

contents of active ingredients and additives. Therefore, their chemical stability is good and their biological activity is relatively high. Poorly water-soluble active ingredients of EC can be sprayed as oil-soluble substances in water since they emulsify spontaneously when diluted (Patzke and Schieber, 2018; Wiwattanapatapee *et al*., 2009). In the present study, ATEC was formulated by comprising of anthraquinone-rich extract, TiO_2 NPs, the by-product of cinnamon oil, surfactants, and propylene glycol. The ATEC has been further fabricated into ATNE spontaneously nanoemulsions by diluting with water.

During the preparation process of ATEC, to avoid the interaction of anthraquinone and TiO_2, the nanoparticles of TiO_2 were capsulated in PEG 400 as previously described in sections 2.2 and 3.2. The TiO_2 NPs showed an average droplet size of 103.9 nm and high stability and were introduced into the preparation process of emulsifiable concentrate at the final stage (Section 2.3). Finally, ATNE was fabricated with ATEC and water under stirring and ultrasonication. The obtained ATNE formulations were employed in material characterization and to test for the control efficacy of ATNE against powdery mildew in the field.

Important metrics for assessing the quality, homogeneity, and dispersibility of nanoemulsions are particle size distribution, mean particle diameter (Z-averages), and polydispersity index (PDI). In the present study, the average ATNE's measured size is 484.4 nm and PDI value was 0.824, indicating a moderate homogeneity for the colloid system. The dispersion stability of ATNE was indicated by a ζ potential value of -25.3 mV (Figure 3). The nanoemulsion droplets of anthraquinone and TiO_2 NPs were stabilized due to the use of surfactants Tween 20 and 60 together with co-solvent PG and the by-product of cinnamon oil, and the steric hindrance helps reduce the degree of collision between droplets. Besides, the morphology and homogeneity of ATNE were observed through SEM measurement. Figure 4 exhibits the images of ATEN (1:400) at magnifications of 3,000×, 5,000× and 15,000× that demonstrated that the colloidal system has a round shape with a range of 147 to 214 nm (Figure 4C) and homogeneity was moderate as determined by DLS.

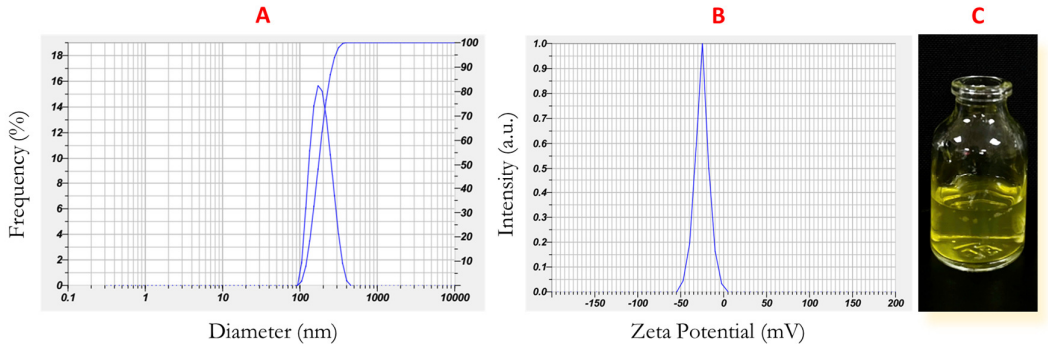

Figure 3. DLS measurement of the distribution of droplet sizes (a) and ζ potential (B), and image of nanoemulsion ATEN (1:400)

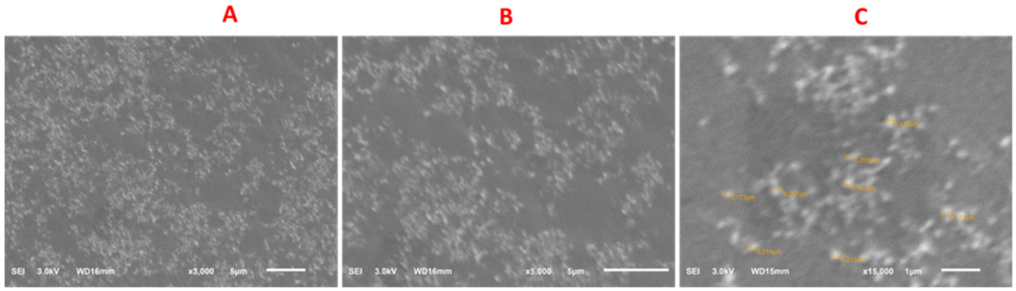

Figure 4. Scanning electron microscopy (SEM) images of ATEN (1:400) under various circumstances: (A) at a magnification of 3,000X, scale bar: 5 μm; (B) at a magnification of 5,000X, scale bar: 5 μm; and (C) at a magnification of 15,000X; scale bar: 1 μm

ATNE's droplet size and form were revealed by a JEOL 2100 TEM analysis at magnifications of 200,000 times. Figure 5 illustrates the range of ATNE droplets, ATNE produced was uniform in size, and spherical in shape, which were 25-35 nm. (Figure 5). The findings of the droplet size study using TEM showed a moderate correlation with those by DLS. The nanoparticle size obtained by TEM is smaller compared to the size observed from DLS analysis, which is entirely consistent. This is because DLS provides dynamic size measurements from a large ensemble of particles, hydrophilic polymers become relatively large, interact with water, and cause the particles to appear larger. Whereas, since TEM only observes a limited area, it only sees a small number of particles and yields a static size. In fact, the observed phenomena are also consistent with a number of previous studies on the differences, advantages, and disadvantages of each method (Filippov *et al*., 2023; Eaton *et al*., 2017).

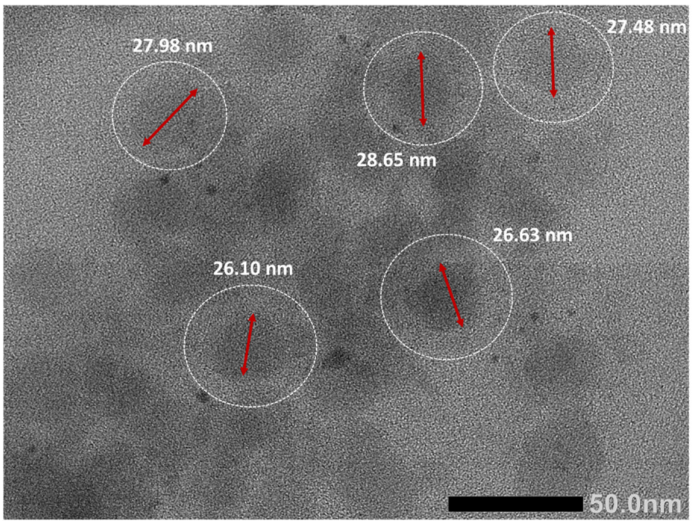

Figure 5. Transmission electron microscopic (TEM) image of ATEN (1:400)
Scale bar: 50 nm

Typical IR bands of emodin, anthraquinone-rich extract (CKC), TiO_2 coated PEG and emulsifiable containing anthraquinone and TiO_2 NPs (ATEC) are presented in Figure 6. In the IR spectrum of emodin, the characteristic peaks of C=O peak at 1620 cm^{-1} ~ 1610 cm^{-1}, and 3482 cm^{-1} proved the presence of hydroxy group. Sharp absorption bands were observed for the anthraquinone carbonyl groups in the spectral region of 1673–1633 cm^{-1}. Broadband with moderately strong intensity centered at 3412 cm^{-1} corresponds to the O-H stretching frequency, while moderate alkyl C-H stretching frequencies were observed at 2939 and 2855 cm^{-1}. The lower frequency region of the spectrum of a slightly broadened intense absorption band at 1633 for the conjugated carbonyl. In the IR spectrum of TiO_2 NPs, the Ti-O bending mode and deformative vibration of Ti-OH stretching mode may be observed at 598 cm^{-1} and 1648 cm^{-1} respectively. The appearance of absorption peaks such as C-O-C (symmetrical valence vibration, 1031 cm^{-1}) and –CH (out-of-plane bending vibration, 1357 cm^{-1}), peaks at 1070 cm^{-1} (C-O-C group), 1298 cm^{-1} (C-O group) and 2860 cm^{-1}(-CH_2 group) shows the interaction of PEG 400 with the TiO_2 nanoparticles (León *et al*., 2017). In the IR spectrum of emulsifiable concentrate containing anthraquinone and TiO_2 NPs (ATEC), the peak at 3400 cm-1 represents the valence vibration of the -OH group of ATEC. The peaks at 1673 cm^{-1} and 1732 cm^{-1} correspond to the deformation vibration of adsorbed water molecules and Ti-OH, respectively. The peak band ~604 cm^{-1} corresponds to the vibrations of Ti-O-Ti, respectively are evidence for the formation of ATEC. Due to the by-product of cinnamon oil (BCO) containing cinnamaldehyde, it also showed the presence of a stretch at 1732 cm^{-1}, which is associated with the cinnamon aldehyde's carbonyl group C=O. Stretches at 1620–1625 cm^{-1} were linked to the alkene group (C=C bond) in the spectrum.

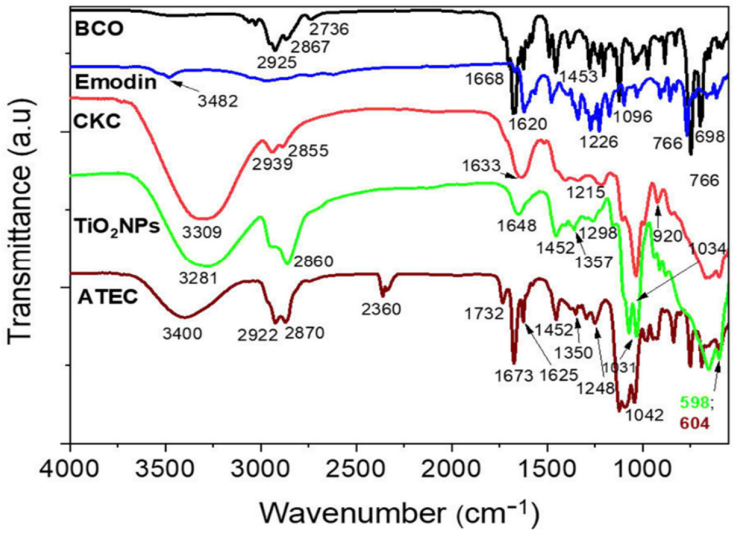

Figure 6. Fournier transforms infrared spectroscopy (FTIR) spectra of by-product of cinnamon oil (BCO), emodin, anthraquinone-rich extract (CKC), and emulsifiable concentrate containing anthraquinone, BCO, and TiO_2 NPs (ATEC)

In vitro antifungal potential of ATEC against various melon phytopathogenic fungi

The *in vitro* antifungal activity of ATEC was tested against *B. cinerea*, *Phytophthora* spp., *F. oxysporum*, *Colletotrichum* spp., *Sclerotium* spp., and *Rhizoctonia* spp. by using poison food technique. The bioassay results showed that ATEC possesses a high antifungal potential against test fungi (Figure 7). The ATEC completely inhibited the mycelial growth of all test fungi 0.125% TO 0.5% at 2 days after treatment. At a concentration of 0.125%, it also suppressed *B. cinerea*, *Phytophthora* spp., *Colletotrichum* spp., *Sclerotium* spp., and *Rhizoctonia* spp. mycelial growths by 100% inhibition; however, the mycelial growth of *F. oxysporum* was inhibited by 76.9 and 70.8% at 4 and 6 days after treatment (Figures 7B to 7D). Contrastingly, at the concentrations of 0.25% and 0.5%, the mycelial growth of all test fungi was completely inhibited by ATEC at 4 and 6 days after treatment (Figure 7A). The mechanism of detoxication of FO could lead to the reduced antifungal effectiveness of ATEC on the mycelial growth of FO at 6 days after treatment. The phenomena have been seen on various phytopathogenic fungi belonging to Fusarium. But in general, the remaining 5 fungi were inhibited completely by ATEC. It could be explained by the occurrence of nanodroplets containing anthraquinone and TiO_2 NP based on cinnamon oil.

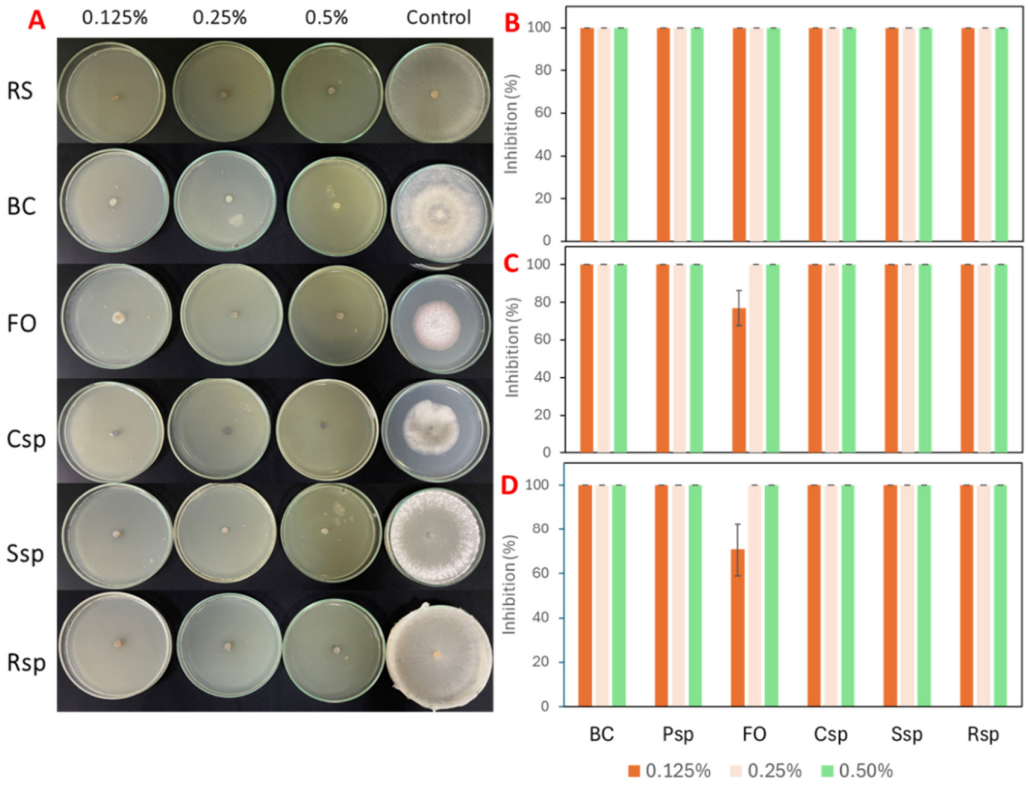

Figure 7. *In vitro* antifungal of ATEC against the mycelial growths of various fungal pathogens

A: the mycelial growth of fungal pathogens treated with ATNE at 6 days after treatment. B: Inhibition (%) of ATNE at 2 days after treatment. C: Inhibition (%) of ATNE at 4 days after treatment. C: Inhibition (%) of ATEC at 6 days after treatment. BC: *Botrytis cinerea*, Psp: *Phytophthora* spp., FO: *Fusarium oxysporum*, Csp: *Colletotrichum* spp., Ssp: *Sclerotium* spp., and Rsp: *Rhizoctonia* spp.

In the *in vitro* bioassay of ATEC against spore germination of *E. cihoracearum*, the formulation was formulated into nanoemulsions of which ATEC and water with the ratio of 1:400 was characterized as stable nanoemulsion formulation ATNE with an average droplet size of 484.4 nm and ζ potential value of -25.3 mV. At 0.5% and 1%, the test formulation inhibited 100% spore germination after 16h. At the lower concentrations of 0.125 and 0.25%, the inhibition of ATEC reduced to 47.33% and 68.67%, respectively (Table 2 and Figure 8).

Table 2. *In vitro* antifungal activity of ATEC against germination of *Erysiphe cihoracearum* spores

No	Concentration (%)	Percentage of germinated spores (%)	Inhibition (%)
1	0.125	52.67 c	47.33 a
2	0.25	31.33 b	68.67 b
3	0.5	0 a	100 c
4	1.0	0 a	100 c
5	Negative control	100 d	-
	LSD 5%	4.04	4.68

Germination of *Erysiphe cihoracearum* spores was observed at 16 h after treatment. Inhibition of ATEC on germination was calculated based on the proportion (%) of spores that did not germinate.

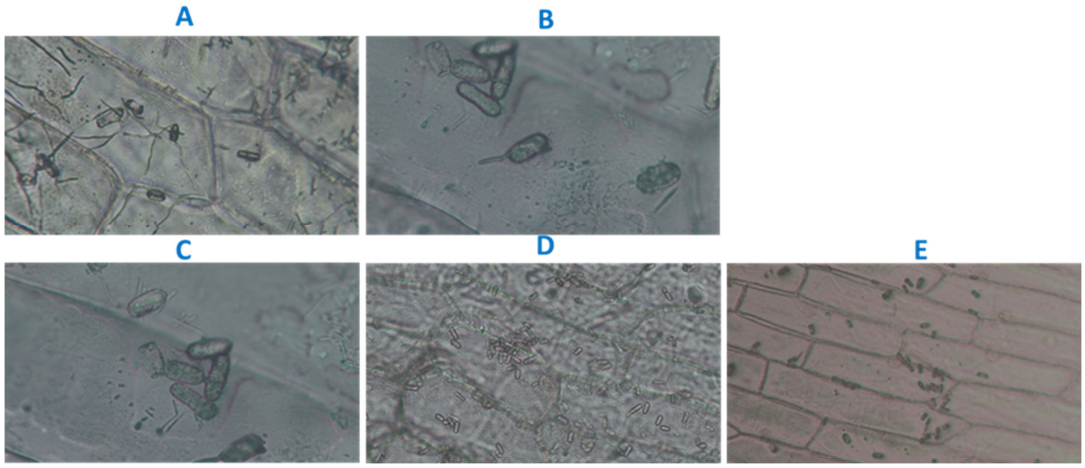

Figure 8. *In vitro* inhibition of ATEC for spore germination of *E. cihoracearum* in 16h. A: negative control; B: 0.125%; C: 0.25%; D: 0.5% and E: 1%

Field assessments of the suppression of ATNE nanoemulsion against powdery mildew in KCN honeydew melon plants

In the *in vitro* bioassay against spore germination of *E. cihoracearum*, ATEC was remarkably active against the test fungus. It effectively inhibited the mycelial growth of *B. cinerea*, *Phytophthora* spp., *Colletotrichum* spp., *Sclerotium* spp., and *Rhizoctonia* spp., and spore germination of *E. cihoracearum* at concentrations higher than 0.125% (equivalent to 800-fold dilution). In the field test, the disease control efficacy of nano ATNE formulations (1:400) and (1:700) were evaluated against powdery mildew. Consequently, they significantly suppressed the DI and DSI of powdery mildew in melon. Of them, ATNE formulation (1:400) caused the best efficacies of 46.5% and 62.34% for powdery mildew in melon at all of the assessments at 5 days and 10 days after spraying, respectively. The 1st assessment 5 days after spraying showed their DI values were significantly lower than those of negative control (15.11%). There were no differences between DI values of ATNE formulations (1:400) and (1:700); however, in the 2nd assessment at 10 days after treatment, DI and DSI of ATNE formulation (1:400) were significantly lower than those of the latter (1:700) (Table 3).

Table 3. Disease assessment and control efficacy of ATNE against powdery mildew caused by *Eryshipe cichorasearum* in the field of KCN honeydew melon

Test materials	Before spray		The 1st assessment (5 days after spray)		CA (%)	The 2nd assessment (10 days after spray)		CA (%)
	DI %	DSI%	DI %	DSI%		DI %	DSI%	
ATNE 1: 400	7.11	1.42	9.33 b	2.04b	46.51 a	11.56 b	2.58 b	62.34 a
ATNE 1: 700	6.67	1.33	9.33 b	2.22b	41.86 b	12.00 b	2.84 b	58.44 ab
Positive control	6.67	1.33	9.78 b	2.20b	41.86 b	12.44 b	2.93 b	57.14 b
Negative control	6.22	1.24	15.11 a	3.86a		20.89 a	6.84 a	
LSD5%			1.88	0.52	2.59	1.68	0.96	4.45

The field test was conducted on 4-week KCN honeydew melon plants in Hai Phong province from March to June 2024. CA: control efficacy (%); DI: disease incidence (%); DSI: disease severity index (%); Positive control was treated with *Chaetomium* sp (10^9 CFU/mL)

The results of the DSI assessment of powdery mildew on KCN melon plants between the treatments of ATNE nanoemulsions through the growth stages showed that powdery mildew appeared on melon in

somewhat levels, but the DI and DSI values were low and the levels of damages were statistically insignificant (Table 3). During the field trial, it was observed that the more the melon plants grew and developed, the rate of powdery mildew gradually decreased. Besides, in the 2nd assessment, ATNE (1:400) caused an insignificant rate of disease occurrence; and its disease control efficacy (62.34%) was significantly higher than that of positive control (57.14%) as shown in Figure 9 and Table 3.

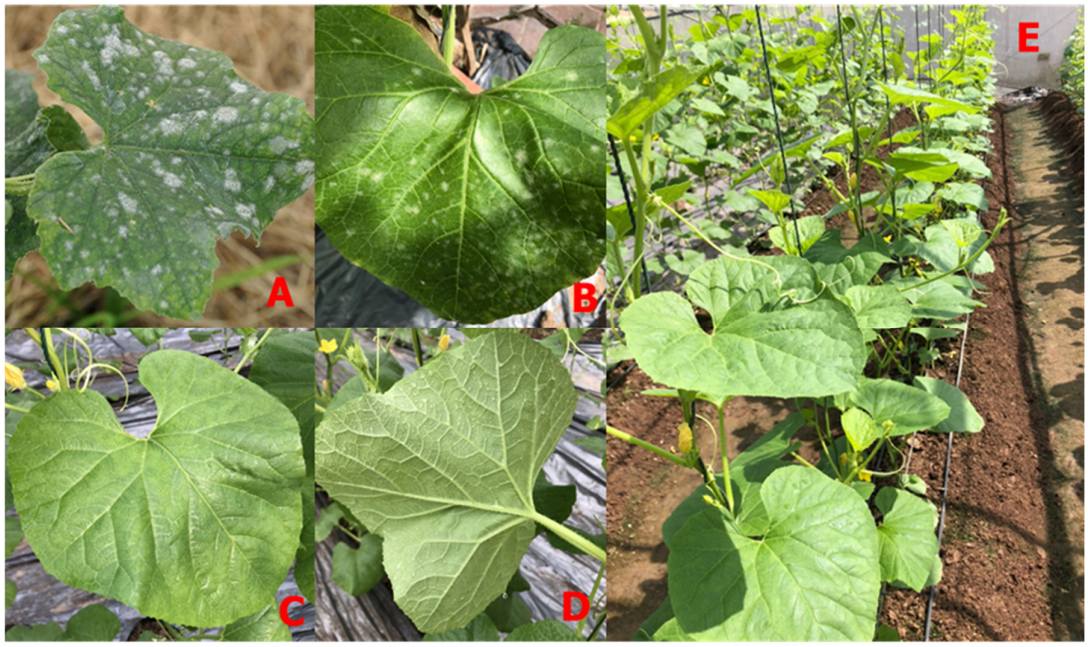

Figure 9. Field testing of ATNE against powdery mildew disease in Kim Co Nuong melon in the testing field
Powdery mildew infection before spray (A) and at 5 days after treatment (B). Images of the upside and backside of melon leaf with no powdery mildew at 10 days after treatment with nanoemulsion ATNE (1:400)

In our previous study on the antifungal activity of anthraquinone from *Rumex chinensis*, the n-Hexane and EtOAc fractions of this plant roots were rich in anthraquinone such as chrysophanol, physion and emodin and strongly suppressed barley powdery mildew (*B. graminis* f. sp. *hordei*) by about 93 to 100% on barley seedlings *in vivo* at concentrations from 333 to 3000 µg/mL (Pham *et al*., 2020). Emodin, physcion, aloe-emodin, and rhein derived from the chloroform soluble fraction of *Cassia tora* seeds showed high to moderate fungicidal activities against *B. cinerea*, *E. graminis*, *P. infestans*, and *R. solani*. At 500 and 1000 µg/mL, they suppressed *R. solani* infection in rice seedlings with control efficacies from 86 to 100% in vivo (Kim *et al*., 2004). According to Liu *et al*. (2009), emodin and chrysophanol were isolated from *Trichoderma harzianum* culture broth and inhibited the mycelial growth of *B. cinerea*, and *R. solani* by 39 to 51.7% at 500 µg/mL. Rodrigues *et al.* (2018) prepared an anthraquinone lapachol nanoemulsion that demonstrated a homogenous size distribution, good physical stability, and droplet size of roughly 70 nm. Nevertheless, to date, no reports of botanical anthraquinone nanoformulations against phytopathogenic fungi that affect melon have been reported. Our investigation of ATNE nanoemulsion of anthraquinone and TiO_2 NPs was the first study on the new material with superior antifungal activity.

Titanium dioxide has been used extensively as a UV absorber for coating applications and is generally accepted as a safe substance in the food and pharmaceutical industries (Ali Alasmary *et al*., 2022; León *et al*., 2017). Applying TiO_2 NPs is a practical way to inhibit pathogenic bacteria and there have been numerous reports of antimicrobial properties of TiO_2 NPs (Arezoo *et al*., 2020). Besides the antifungal potential of

anthraquinone against phytopathogenic fungi, TiO_2 NPs also played a critical role in triggering plant resistance to fungal infection and directly inhibiting pathogenic fungi (Satti *et al*., 2022; Alasmary *et al*., 2022; Vatankhah *et al*., 2023). The nano droplets of anthraquinone and TiO_2 may occur together on the leaf surface or penetrate the cells of leaves or fungi. This may lead to an interaction between anthraquinone and TiO_2. According to Trochowski *et al*. (2023), 1,5, 1,8-dihydroxyanthraquinones (DHAQ) are the most active and stable modifiers of TiO_2. The anthraquinone triggered the photocatalysis process in TiO_2. When DHAQ/TiO2 is exposed to visible light, photocatalysis occurs, generating free radicals such as hydroxyl radicals (•OH) and superoxide anions ($O_2^{\bullet-}$). Consequently, these free radicals have the ability to destroy the cell membrane of microorganisms, leading to the destruction or inhibition of microbial growth (Trochowski *et al*., 2023).

In the present study, the innovative points of ATEN are that the formulation was composed of low-content anthraquinone extract and TiO_2 NPs in ATNE (1:400); however, it displayed excellent antifungal effectiveness. According to previous reports, the characteristics and physiochemical properties of nanoemulsions could lead to an enhancement of their antimicrobial efficacy against various microorganisms (Arezoo *et al*., 2020; Yi *et al*., 2021; Younis *et al*., 2023). In addition, plant-based essential oils are recognized as a safe source of antimicrobial substances (Elsalam and Khokhlov, 2015; Mostafa *et al*., 2021). Of those, cinnamon essential oil has been considered as GRAS and demonstrates antimicrobial, antioxidant, and antifungal properties (Pandey *et al*., 2017). In this study, the by-product of cinnamon oil used as an additive could contribute to the oily phase of droplets and also partly cause the inhibition of fungi. The evidence of antifungal efficacy of ATNE was clearly proved through both in vitro bioassay and field tests. By using in vitro bioassay, our study has provided insight into the mode of action of ATNE could be explained through the inhibition of the nanoformulation for spore germination *E. cihoracearum*. In the future, to identify possible adverse effects, toxicological testing in animals of ATEN should be conducted. The interaction of ATNE on the hyphae of *E. cihoracearum* also should be observed by microscopy and biochemical assays to further determine the other mode of action for ATNE. Furthermore, the chemical interaction of anthraquinone and TiO_2 may happen during their permeation actions in plant cells, lead to promote the photocatalysis processes, and may cause an enhancement of antifungal efficacy of ATNE against various fungal pathogens in melon, for example of downy mildew. The probability of this interaction should be examined by planta test in the future.

Conclusions

The nanoemulsion of anthraquinone and TiO_2 NPs showed superior antifungal potent against the causal agents of melon fungal diseases. The nanoemulsion ATNE was prepared by incorporating anthraquinone and TiO_2 NPs (103.9 nm), tween 20 and 60 together with cosolvent PG showed an average droplet size of 484.4 nm and salability with ζ potential value of -25 mV. The morphology of ATNE nanodroplets observed using SEM and TEM showed that ATNE droplets were spherical in shape. The ATNE effectively suppressed the powdery mildew in melon by 62.34% at a 10-day assessment after spray. The development of melon plants was found to be normal and no phytotoxic symptom was observed. Our findings suggested that ATNE could be used effectively to control powdery mildew in melon. In the future, the assessment of ATNE against powdery mildew in melon needs to be verified on various melon cultivars and the winter season too.

Authors' Contributions

D.Q.P, H.V.D, Q.D.L and L.D.T: Funding acquisition, conceptualization, methodology, investigation, review, and editing; Q.D.L, H.T.P and H.D.V: Conceptualization, methodology, investigation, formal

analysis, data curation, writing original draft, review, and editing; T.Q.D, T.V.C and D.Q.P: Conceptualization, investigation, review, and editing; T.T.L; H.K.N and A.T.K.V: Formal analysis, data curation, K.N.T: Resources, review, and editing; S.V.N: Review, and editing; T.Q.D: Investigation; Q.D.L and H.V.D: Supervision. All authors read and approved the final manuscript.

Ethical approval (for researches involving animals or humans)

Not applicable.

Acknowledgements

This work was funded by project number UDNDP.06/2022-2023 from the VAST and Department of Science and Technology of Hai Phong, Vietnam.

Conflict of Interests

The authors declare that there are no conflicts of interest related to this article.

References

Alasmary FA, Rajaram SK, Rajabathar J, Innasimuthu GM, Sankar K, Stephen MS, AlKahtani AMA, Salem AA, Mohammed AH (2022). Titanium dioxide nanoparticles fabrication from *Parmotrema austrosinense* (Zahlbr.) Hale extracts and its antimicrobial efficacy against plant pathogens. Inorganic Chemistry Communications 145:110007. *https://doi.org/10.1016/j.inoche.2022.110007*

Al-Sahli SA, Al-Otibi F, Alharbi RI, Amina M, Al Musayeib NM (2024). Silver nanoparticles improve the fungicidal properties of *Rhazya stricta* decne aqueous extract against plant pathogens. Scientific Reports 14:1297. *https://doi.org/10.1038/s41598-024-51855-5*

Arezoo E, Mohammadreza E, Maryam M, Abdorreza MN (2020). The synergistic effects of cinnamon essential oil and nano TiO_2 on antimicrobial and functional properties of sago starch films. International Journal of Biological Macromolecules 157:743-751. *https://doi.org/10.1016/j.ijbiomac.2019.11.244*

Azmi NAN, Elgharbawy AAM, Salleh HM, Moniruzzaman M (2022). Preparation, characterization and biological activities of an oil-in-water nanoemulsion from fish by-products and lemon oil by ultrasonication method. Molecules 27:6725. *https://doi.org/10.3390/molecules27196725*

Bui VC, Le TT, Nguyen TH, Pham NT, Vu HD, Nguyen XC, De Tran Q, Hoang T, Le Dang Q, Lam TD (2021). Curcumin-removed turmeric oleoresin nano-emulsion as a novel botanical fungicide to control anthracnose (*Colletotrichum gloeosporioides*) in litchi. Green Processing and Synthesis 10:729-741. *https://doi.org/10.1515/gps-2021-0071*

Chung A, Trang TNQ, Nguyen T (2022). Evaluation of pests and diseases, yield and quality of some imported melon varieties (*Cucumis melo* L.) under greenhouse conditions (in Vietnamese). Tay Nguyen Journal of Science 16. *https://doi.org/10.5281/zenodo.7324272*

Cui L, Siskos L, Wang C, Schouten HJ, Visser RGF, Bai Y (2022). Breeding melon (*Cucumis melo*) with resistance to powdery mildew and downy mildew. Horticultural Plant Journal, Advances of Cucurbitaceae Research 8:545-561. *https://doi.org/10.1016/j.hpj.2022.07.006*

Dinh TH, Pham TH, Tran DL, Le TT, Vu TT, Nguyen TPT, Le DQ (2021). Study on the effect of integrating endophyte *Bacillus substilis* GB03 and silica nanoparticles on the growth of melon crop (*Cucumis melo*). Vietnam Journal of Science and Technology-Part B 63:33-38. *https://doi.org/10.31276/VJST.63(2).33-38*

Eaton P, Quaresma P, Soares C, Neves C, Almeida MP, Pereira E, West P (2017). A direct comparison of experimental methods to measure dimensions of synthetic nanoparticles. Ultramicroscopy 182:179-190. *http://dx.doi.org/10.1016/j.ultramic.2017.07.001*

Elagamey E, Abdellatef MAE, Haridy MSA, Abd El-aziz ESAE (2023). Evaluation of natural products and chemical compounds to improve the control strategy against cucumber powdery mildew. European Journal of Plant Pathology 165:385-400. *https://doi.org/10.1007/s10658-022-02612-9*.

Elsalam KA, Khokhlov AR (2015). Eugenol oil nanoemulsion: antifungal activity against *Fusarium oxysporum* f. sp. *vasinfectum* and phytotoxicity on cottonseeds. Applied Nanoscience 5:255-265. *https://doi.org/10.1007/s13204-014-0398-y*

Filippov SK., Khusnutdinov R, Murmiliuk A, Inam W, Zakharova LY, Zhang H and Khutoryanskiy VV. (2023). Dynamic light scattering and transmission electron microscopy in drug delivery: a roadmap for correct characterization of nanoparticles and interpretation of results. Materials Horizons 10:5354. *https://doi.org/10.1039/D3MH00717K*.

Hirata K (1942). On the shape of germ tubes of Erysiphaceae (in Japanese with English summary). Bulletin of the Chiba College of Horticulture 5:34-49.

Huang Y, Liang Y, Chen Y, Xiong Q, Li X, Li J, Wang L, Cui J (2024). Emamectin-sodium alginate nano-formulation based on charge attraction with highly improved systemic translocation and photolysis resistance. International Journal of Biological Macromolecules 254:127996. *https://doi.org/10.1016/j.ijbiomac.2023.127996*

Ke J, Li MT, Xu S, Ma J, Liu MY, Han Y (2023). Advances for pharmacological activities of *Polygonum cuspidatum* - A review. Pharmaceutical Biology 61:177-188. *https://doi.org/10.1080/13880209.2022.2158349*

Kim YM, Lee CH, Kim HG, Lee HS (2004). Anthraquinones isolated from *Cassia tora* (*Leguminosae*) seed show an antifungal property against phytopathogenic fungi. Journal of Agricultural and Food Chemistry 52:6096-6100. *https://doi.org/10.1021/jf049379p*

Le TT, Nguyen HD, Ho DQ, Phan THT, Tran PC, Dinh TTG, Le TTH, Ho TN, Nguyen TT, Tran LD, Le DQ (2024). Synthesis and evaluation of copper oleate nanoparticles against citrus anthracnose caused by *Colletotrichum gloeosporioides*: *In situ* experiments, *in vitro* bioassays, and field trials. Chemistry Select 9:e202401735. *https://doi.org/10.1002/slct.202401735*

León A, Reuquen P, Garín C, Segura R, Vargas P, Zapata P, Orihuela PA (2017). FTIR and Raman characterization of TiO_2 nanoparticles coated with polyethylene glycol as carrier for 2-Methoxyestradiol. Applied Sciences 7:49. *https://doi.org/10.3390/app7010049*

Liu SY, Lo CT, Shibu MA, Leu YL, Jen BY, Peng KC (2009). Study on the anthraquinones separated from the cultivation of *Trichoderma harzianum* Strain Th-R16 and their biological activity. Journal of Agricultural and Food Chemistry 57:7288-7292. *https://doi.org/10.1021/jf901405c*

Mostafa YS, Hashem M, Alshehri AM, Alamri S, Eid EM, Ziedan ESHE, Alrumman SA (2021). Effective management of cucumber powdery mildew with essential oils. Agriculture 11:1177. *https://doi.org/10.3390/agriculture11111177*

Pandey AK, Kumar P, Singh P, Tripathi NN, Bajpai VK (2017). Essential oils: sources of antimicrobials and food preservatives. Frontiers in Microbiology 7. *https://doi.org/10.3389/fmicb.2016.02161*

Patzke H, Schieber A (2018). Growth-inhibitory activity of phenolic compounds applied in an emulsifiable concentrate - ferulic acid as a natural pesticide against *Botrytis cinerea*. Food Research International 113:18-23. *https://doi.org/10.1016/j.foodres.2018.06.062*

Pham DQ, Han JW, Dao NT, Kim JC, Pham HT, Nguyen TH, Nguyen NT, Choi GJ, Vu HD, Le Dang Q (2020). *In vitro* and *in vivo* antimicrobial potential against various phytopathogens and chemical constituents of the aerial part of *Rumex chinensis* Campd. South African Journal of Botany 133:73-82. *https://doi.org/10.1016/j.sajb.2020.07.006*

Rodrigues FVS, Diniz LS, Sousa RMG, Honorato TD, Simão DO, Araújo CRM, Gonçalves TM, Rolim LA, Goto PL, Tedesco AC, Siqueira-Moura MP (2018). Preparation and characterization of nanoemulsion containing a natural naphthoquinone. Quimica Nova 41:756-761. *https://doi.org/10.21577/0100-4042.20170247*

Saka A, Shifera Y, Jule LT, Badassa B, Nagaprasad N, Shanmugam R, Priyanka DL, Seenivasan V, Ramaswamy K (2022). Biosynthesis of TiO_2 nanoparticles by Caricaceae (Papaya) shell extracts for antifungal application. Scientific Reports 12:15960. *https://doi.org/10.1038/s41598-022-19440-w*

Satti SH, Raja NI, Ikram M, Oraby HF, Mashwani ZUR, Mohamed AH, Singh A, Omar AA (2022). Plant-based titanium dioxide nanoparticles trigger biochemical and proteome modifications in *Triticum aestivum* L. under biotic stress of *Puccinia striiformis*. Molecules 27:4274. *https://doi.org/10.3390/molecules27134274*

Thanh TTL, Nguyen VL, Pham V.T, Yukio S (2015). Identification of powdery mildew fungus *Erysiphe quercicola* S.Takam & U.Braun causing white feces disease on rubber trees in Vietnam. Journal of Plant Protection Institute 59:43-47. *https://doi.org/10.31276/VJSTE.59(2).43*

Trochowski M, Kobielusz M, Pucelik B, Dąbrowski JM, Macyk W (2023). Dihydroxyanthraquinones as stable and cost-effective TiO_2 photosensitizers for environmental and biomedical applications. Journal of Photochemistry and Photobiology A: Chemistry 438:114517. *https://doi.org/10.1016/j.jphotochem.2022.114517*

Vatankhah A, Aliniaeifard S, Moosavi-Nezhad M, Abdi S, Mokhtarpour Z, Reezi S, Tsaniklidis G, Fanourakis D (2023). Plants exposed to titanium dioxide nanoparticles acquired contrasting photosynthetic and morphological strategies depending on the growing light intensity: a case study in radish. Scientific Reports 13:5873. *https://doi.org/10.1038/s41598-023-32466-y*

Vietnam National Standard Number TCVN 12561:2022 (2022). Pesticides- Bio-efficacy field trials. Ministry of Science and Technology of Vietnam.

Vietnam Sector Standard Number 10TCN 333:1998 (1998). Regulations for efficacy testing of plant protection products for controlling powdery mildew affecting cucurbit plants in the field. Ministry of Agriculture and Rural Development.

Wiwattanapatapee R, Sae-Yun A, Petcharat J, Ovatlarnporn C, Itharat A (2009). Development and evaluation of granule and emulsifiable concentrate formulations containing *Derris elliptica* extract for crop pest control. Journal of Agricultural and Food Chemistry 57:11234-11241. *https://doi.org/10.1021/jf901862z*.

Yi L, Zhao R, Li Y, Zhou Z (2021). Limonin enhances the antifungal activity of eugenol nanoemulsion against *Penicillium italicum in vitro* and *in vivo* tests. Microorganisms 9:969. *https://doi.org/10.3390/microorganisms9050969*.

Younis AB, Milosavljevic V, Fialova T, Smerkova K, Michalkova H, Svec P, Antal P, Kopel P, Adam V, Zurek L, Dolezelikova K (2023). Synthesis and characterization of TiO_2 nanoparticles combined with geraniol and their synergistic antibacterial activity. BMC Microbiology 23:207. *https://doi.org/10.1186/s12866-023-02955-1*

The journal offers free, immediate, and unrestricted access to peer-reviewed research and scholarly work. Users are allowed to read, download, copy, distribute, print, search, or link to the full texts of the articles, or use them for any other lawful purpose, without asking prior permission from the publisher or the author.

License - Articles published in ***Notulae Botanicae Horti Agrobotanici Cluj-Napoca*** are Open-Access, distributed under the terms and conditions of the Creative Commons Attribution (CC BY 4.0) License.

© Articles by the authors; Licensee UASVM and SHST, Cluj-Napoca, Romania. The journal allows the author(s) to hold the copyright/to retain publishing rights without restriction.

Notes:

- Material disclaimer: The authors are fully responsible for their work and they hold sole responsibility for the articles published in the journal.
- Maps and affiliations: The publisher stay neutral with regard to jurisdictional claims in published maps and institutional affiliations.
- Responsibilities: The editors, editorial board and publisher do not assume any responsibility for the article's contents and for the authors' views expressed in their contributions. The statements and opinions published represent the views of the authors or persons to whom they are credited. Publication of research information does not constitute a recommendation or endorsement of products involved.